THE EFFECT OF MICROSTRUCTURE ON APPEARANCE OF FATIGUE FRACTURE OF H I STEEL

J.Woodtli-Folprecht*, M.Prodan**

Fluctuating tension fatigue tests of ferritic-pearlitic steel HI were conducted under R=0.3. The measured propagation rate was correlated to the calculated crack growth rate based on striation spacing. The microfractographical method shows higher propagation rates in the vicinity of the treshold value of ΔK_0.This increase of cracking rate can be traced to local different microscopical fracture mode. Based on the examination of a metallographical section, the morphology of the fracture surface could be related to the individual constituents of the structure.

INTRODUCTION

When dealing with fractures which have occurred in ferritic-pearlitic steels in service, it is often difficult to distinguish between static or overload fractures on the one hand and fatigue fractures on the other. Particularly in the areas with pearlite grains, one often detects striated structures which are similar to fatigue striations. The local morphology of the fracture depends not only on the type and intensity of the stress to which the metal is subjected, but also on the structure of the metal. The object of this test was to obtain information on the fracture appearance characteristics as a function of the structure constituents and of the stress conditions.

MATERIAL

The test material selected was a type H I (DIN 1.0345) boiler plate steel with a tensile strength of 400 N/mm^2 and an elastic limit of 220 N/mm^2. It was present in the normalized condition. The ferritic-pearlitic microstructure is shown in Figure 1. Its chemical composition is as follows:

C = 0.16 P_{max} = 0.05

Si = 0.35

Mn = 0.4 S_{max} = 0.05

* Swiss Federal Laboratories for Materials Testing and Research, Dübendorf

** Swiss Federal Institute for Reactor Research, Würenlingen

The test material was present in the form of metal sheet with a thickness of 4 mm.

SPECIMENS

The fatigue tests were carried out with flat specimens of the following dimensions: 300 mm by 100 mm by 4 mm. The longitudinal axes of the test pieces were identical with the direction in which the sheet had been rolled, so that the direction of crack propagation was at right angles to the direction of rolling. In order to accelerate the initiation of the cracks, the specimens were provided with a two-sided pre-notched hole. The nominal area in each case was 288 mm^2.

TEST PROCEDURE

The specimens were fatigued with a maximum force of 60 kN in a testing device consisting of an "Amsler" load frame with a type "GCS" servo-hydraulic actuator. All the test pieces were stressed in the fluctuating tension range with a test frequency of 5 to 10 Hz and an R-factor of 0.3. To detect the overload fracture when it occurred, a crack wire was used.

During the crack propagation phase, the progression of the crack was observed and measured by means of a microscope.

The longer fatigue fracture surface of each fractured specimen was examined in a SEM. Each fracture surface was searched for areas with fatigue striations. Furthermore, the distance of these areas from the fracture beginning and density of striations was estimated.

The next objective was to determine the influence of the microstructure on the propagation of the cracks. For this purpose, part of the fatigue fracture surface of specimen no. 3 was examined fractographically as well as metallographically along a line running parallel to the crack propagation direction. The metallographic section was made perpendicular to the fracture surface, allowing an accurate correlation to be established between the fracture characteristics and the microstructure (see Figure 9).

RESULTS

Secondary Cracks

As one follows the fracture surface topography from the starting point of the fracture up to the residual fracture, the structure of the fracture surface will be seen to become somewhat coarser, and the number and depth of the secondary cracks increases. All this is the result of the increase in the dynamic stress intensity factor. Two types of secondary cracks were established. The mostly gaping, coarser cracks are often the result of a separation at the grain boundaries, and their paths are independent of the crack propagation direction (see Figure 2). The fine secondary cracks run parallel to the fatigue striations, and thus give

us a glue as to the local propagation of the fatigue crack (see Figure 3).

According to reference (5), the propagation mechanism of the secondary cracks is similar to that of the main crack. The fact that in our test, too, fatigue striations were found in some places on the flanks of the secondary cracks can be taken as a corroboration of this.

Fatigue Striations

In the micron range, the fatigue fracture will spread in irregularly arranged fracture paths (see Figure 4).

In a lot of areas, fatigue striations can be detected normal to the direction of local fracture propagation. The direction in which the fatigue striations run varies from one fracture path to another. Figure 2 clearly shows that the size of the individual fracture paths is independent of - that is to say larger than - the grain size of the material. According to Laird (1), the fatigue striations can be considered ductile. While in some areas the structure of the fatigue striations is fairly regular (see Figure 5), forms such as shown in Figure 6 can be found in many other parts. The more or less regular fatigue striations occur mainly in the ferrite grains. The irregular striations, on the other hand, are probably often correlated with the pearlite grains. Furthermore, it was established that the fracture surface within a pearlite grain frequently presents a smooth, structureless topography (see Figure 7).

According to Cooke and Beevers (2), these areas are associated with the course of the cracks along a cementite lamella in the boundary region between the ferrite and the cementite within a pearlite grain, or with a grain boundary between a ferrite and a pearlite grain. The frequent zones exhibiting an irregular striation structure can also be attributed to the fact that the fracture runs through a perlite grain, and these areas often reflect the structure of cementite lamellae.

CORRELATION BETWEEN MICROSCOPICAL AND MACROSCOPICAL CRACK GROWTH RATE

In order to establish the correlation between the microscopical and the macroscopical fatigue crack growth rate, microfractographical results were compared with computed da/dN. The method for computing da/dN involves fitting a second-order polynomial (parabola) to successive sets of (N,a) data points.

The value of ΔK associated with a da/dN value is computed using the fitted half crack length a_{reg} and equations as follows:

$$\Delta K = \sqrt{\Delta\sigma\ \Pi a_{reg}} \cdot \sqrt{\sec \frac{\Pi a_{reg}}{W}} \qquad (1)$$

$$\Delta\sigma = \frac{F_{max} - F_{min}}{W \cdot B} \qquad (2)$$

In the evaluated cases the correction function $f(a/W) = (\sec (\pi a/W)^{1/2}$ has values in the interval $1.03 \leq f(a/W) \leq 1.2$.

The results marked by solid symbols in Figure 8 are in better agreement with ASTM E 647-81 (3) than those marked by open symbols. In part, the open symbols were evaluated graphically (4) and in one case they mark an interval with a load change.

The half open symbols in Figure 8 have been determined using striation spacing measurements obtained from the fracture surface. As the result shows, the microfractographical method shows higher propagation rates especially in the vicinity of the treshold value of ΔK_0.This increase of propagating rate can be traced to local different micromechanism of fracture.

SYMBOLS USED

a = crack length (mm)

a_{reg} = half crack length (mm)

ΔK = stress intensity range ($N\ mm^{-3/2}$)

$\Delta\sigma$ = applied stress amplitude ($N\ mm^{-2}$)

r = fatigue striation spacing (mm/cycle)

F = load (N)

W = specimen width (mm)

B = specimen thickness (mm)

$\sec x = \frac{1}{\cos x}$

$R = \frac{\sigma_{min}}{\sigma_{max}}$

REFERENCES

1. Laird,C., 1966, "Fatigue Crack Propagation", ASTM STP No. 415, Philadelphia.

2. Cooke,R.J., and Beevers,C.J., 1974, "Slow Fatigue Crack Propagation in Pearlitic Steels", Mat.Sci.Eng.13, 201-210.

3. Annual Book of ASTM Standards, Part 10, 1981, (E 647-81), 763-783.

4. Tada,H., Paris,P.C., and Irwin,G.R., 1973, "The Stress Analysis of Cracks Handbook", Del Research Corp., 2.1-2.3.

5. Gauthier,P., de Rabandy,H., and Anvient, I., 1975, EFM Vol.5, 977.

Figure 1 Ferritic-pearlitic microstructure

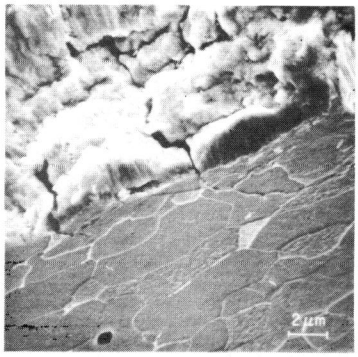

Figure 2 Coarse cracks corresponding with grain bounderies

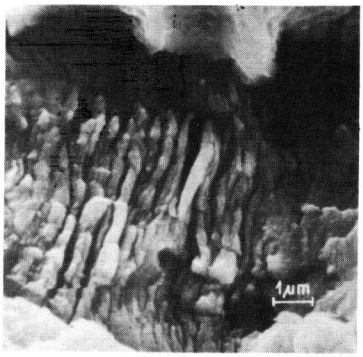

Figure 3 Fine cracks parallel to fatigue striations

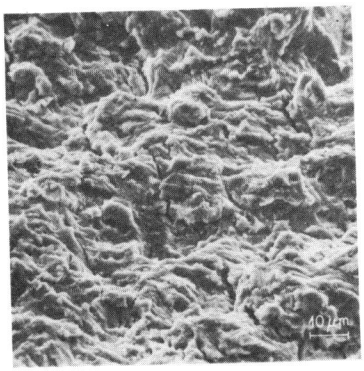

Figure 4 Irregularly arranged fracture paths

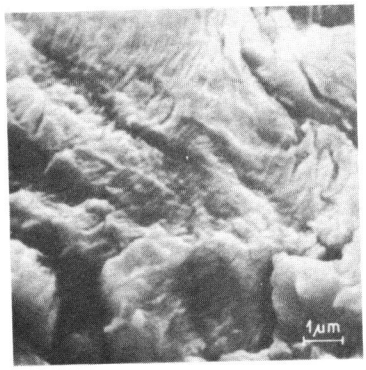

Figure 5 Regular shaped fatigue striations

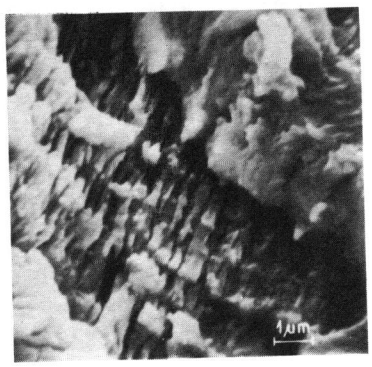

Figure 6 Irregular shaped fatigue striations

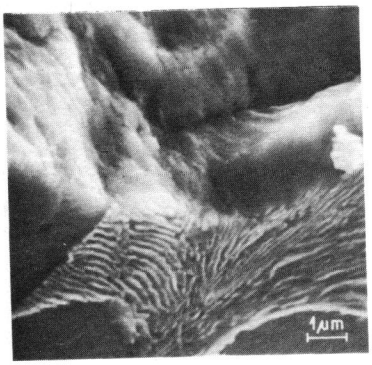

Figure 7 Fracture topography within the pearlit grain

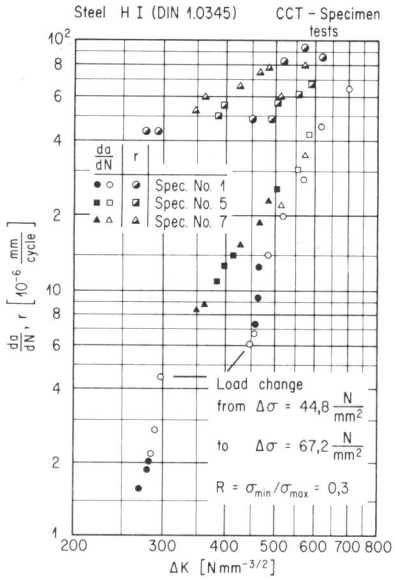

Figure 8 da/dN and striation spacing related to ΔK

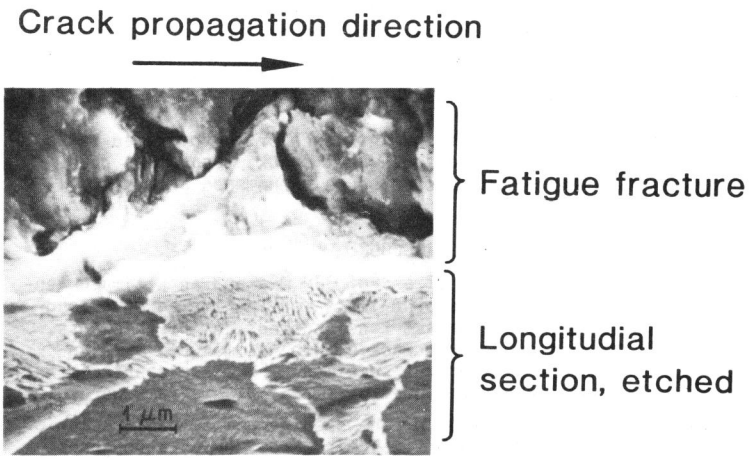

Figure 9 Metallographic section perpendicular to the fracture